

Constraining the Capacity of Global Croplands to CO₂ Drawdown via Mineral Weathering

Fatima Haque,[§] Reza Khalidy,[§] Yi Wai Chiang, and Rafael M. Santos*



Cite This: ACS Earth Space Chem. 2023, 7, 1294–1305



Read Online

ACCESS |

Metrics & More

Article Recommendations

Supporting Information

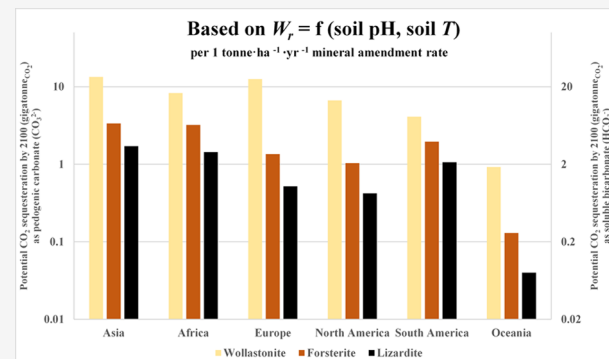
ABSTRACT: Terrestrial enhanced weathering of alkaline silicate minerals is a promising climate change mitigation strategy with the potential to limit the global temperature rise. The formation and accumulation of pedogenic carbonate and bicarbonate in soils/subsoils and groundwater offers a large sink for C storage; the amount of soil inorganic carbon (SIC) presently held within soils has been estimated to be 720–950 Gt of C. These values can be augmented by the addition of a variety of calcium and magnesium silicates via enhanced weathering. While the concept of the application of finely milled silicate rocks for faster weathering rates is well established, there has been limited discussion on the role of local climate, natural SIC content (i.e., the SIC innately present in the soil), and soil pH (among other important agronomic factors) on silicate weathering when applied to croplands, especially in view that the aim is to establish terrestrial enhanced weathering as a carbon dioxide removal (CDR) strategy on a global scale. In this work, we emphasized the importance of soil pH and soil temperature on silicate weathering and looked to estimate an upper limit of (i.e., constrain) the global capacity until the year 2100 for enhanced rock weathering (ERW) to draw down CO₂ in the form of accumulated pedogenic carbonate or soluble bicarbonate. We assessed the global spatial distribution of cropland soil pH, which serves as a proxy for local innate SIC; annual rate of pluvial (rainfall) precipitation; and soil temperature, and found that the potential CO₂ drawdown difference between faster and slower weathering silicates is narrower in Asia, Africa, and South America, while the gap is larger for Europe, North America, and Oceania.

KEYWORDS: enhanced rock weathering, soil remineralization, soil carbon, soil inorganic carbon, alternative liming materials

1. INTRODUCTION

Atmospheric carbon dioxide is rising rapidly because of anthropogenic activities, thus leading to global warming.^{1–3} To limit the global temperature rise to 1.5–2 °C by 2100, as set by the Paris Agreement, there is a pressing need for the timely large-scale implementation of carbon dioxide removal (CDR) strategies.⁴ A promising CDR strategy is terrestrial enhanced weathering, which is based on an acceleration of the natural weathering process, whereby pulverized rock is applied onto land, wherein soils are able to enhance the dissolution of the rocks, and CO₂ is sequestered through pedogenic carbonate (PC) accumulation and/or aqueous bicarbonate formation (i.e., alkalinity enhancement).^{5–9}

Soil inorganic carbon (SIC) is formed mainly through the reactions in eq 1 – 3. First, CO₂ reacts with H₂O to form a bicarbonate ion (HCO₃[–]) and a proton (H⁺) (eq 1). Second, the alkaline earth metal ion (M²⁺) is liberated from silicate minerals by the proton (eq 2), and it ultimately reacts with the bicarbonate to precipitate as a metal carbonate (MCO₃) (eq 3).^{10,11} While this is the conventional route of the silicate mineral carbonation in soil, in regularly irrigated agricultural



soil or the case of high pluvial precipitation (i.e., rainfall), metal carbonate may not precipitate: the reason being that solubility increases significantly as the pH drops below ~6–8 at ambient conditions and is accentuated by the presence of salts. In this case, rather than remaining in the soil profile, the ions (M²⁺, HCO₃[–]) gradually leach into the groundwater and eventually into the oceans where they will eventually precipitate under alkaline conditions and biological assistance as magnesium or calcium carbonates (eq 4).^{11,12} Along the path from point of application to final sink, Dietrich et al.¹³ remind us that secondary carbonate formation should not be neglected in chemical weathering calculations because of what they refer to as “geochemical cascade.” They explain that “elements do not travel directly from the substratum to the rivers through

Received: December 4, 2022

Revised: May 22, 2023

Accepted: May 23, 2023

Published: June 9, 2023



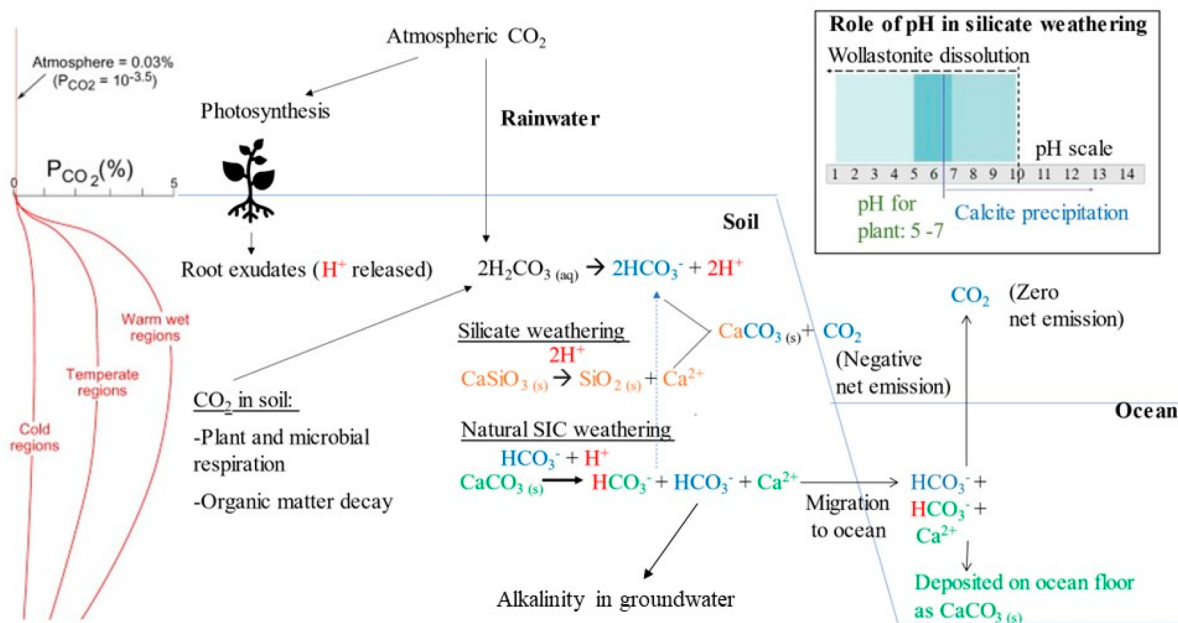
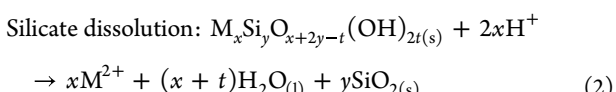
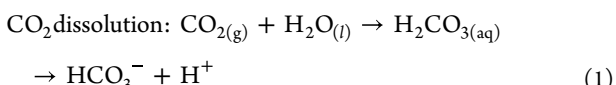
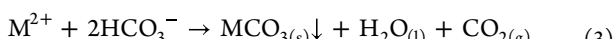


Figure 1. Fate of SIC, both innate SIC and PC, formed as a result of amended silicate weathering. Wollastonite weathering is shown here to explain the mineral carbonation process in soil. Climatic and atmospheric factors (pluvial precipitation and P_{CO_2}) cause an increase in the carbonic acid in the soil system, which speciate with the calcium ions as soluble bicarbonate and, when saturated, precipitate as calcium carbonate (an overall process that still results in negative net emission since 2 mol of CO_2 are consumed and 1 mol of CO_2 is released). Excessive pluvial precipitation also controls the fate of PC (calcite), which can revert to soluble alkalinity (bicarbonate) and occupy the transient groundwater sink before eventually migrating to the ocean where it is also accumulates as added alkalinity in dissolved state before, over a longer time scale, being deposited on the ocean floor as calcium carbonate accompanied by CO_2 degassing (a process resulting in zero net emission). Because protons (H^+) are involved in both the silicate weathering and SIC weathering reactions, soil and subsoil pH are important controlling factors in pedogenic SIC accumulation and migration.

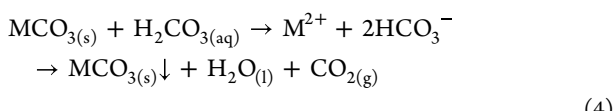
weathering, because some of them can be trapped in terrestrial secondary deposits for an undetermined time."



PC precipitation from accumulated alkalinity (Alk):



PC/Alk migration from soil, via groundwater, to ocean:



For terrestrial enhanced weathering applications, candidate materials are calcium and magnesium silicates, including the olivine solid solution $[(Mg,Fe)_2\text{SiO}_4]$ of the forsterite ($Mg_2\text{SiO}_4$) and fayalite ($Fe_2\text{SiO}_4$) minerals, the pyroxene group $[(Ca,Na,Fe^{II},Mg)(Cr,Al,Fe^{III},Mg,Mn,Ti,V)\text{Si}_2\text{O}_6]$ minerals, such as wollastonite ($Ca_2\text{Si}_2\text{O}_6$) and enstatite ($Mg_2\text{Si}_2\text{O}_6$), and the serpentine group $[(Mg,Fe^{II})_3\text{Si}_2\text{O}_5(\text{OH})_4]$ minerals.¹⁴ Global reserves of peridotite (olivine and pyroxenes) and serpentine are estimated to be sufficient to sequester all carbon that may be emitted from the presently recognized reserves of coal, petroleum, and

natural gas.¹⁵ Known reserves of wollastonite are far more limited, but distributed globally, and have already found application as an agricultural soil amendment for various crops.¹⁶

The silicate dissolution reaction (eq 2) is the weathering rate-limiting step¹⁷ controlled by reaction kinetics and mass transport, whereas the carbonate precipitation/dissolution reactions are thermodynamically controlled.¹⁸ The release of Ca and Mg from the silicate minerals in soil depends on the weathering/dissolution rate, which in turn, depends on several parameters, including temperature and soil pH.¹⁹ With the aim of further acceleration of the weathering rate, the specific surface area of the mineral, directly related to particle size, is also critical.^{20,21} In our previous work,²² the weathering rate of silicate minerals was used to assess the CO_2 sequestration potential of alkaline minerals applied to agricultural soils using an idealized shrinking core model. It was concluded that a particle size smaller than $50 \mu\text{m}$ is needed to accelerate the dissolution rate of forsterite to levels that can contribute significantly to CO_2 sequestration within a 10 year period.

While the concept of the application of finely milled silicate rocks for faster weathering rates is well established, there has been limited discussion on the role of local climate, natural SIC content (i.e., the SIC innately present in the soil), and soil pH (among other important agronomic factors) on silicate weathering when applied to croplands, especially in view that the aim is to establish terrestrial enhanced weathering as a CDR strategy on a global scale. Therefore, this perspective emphasizes the importance of soil pH and soil temperature on silicate weathering and looks to constrain (i.e., estimate an upper limit on the basis of the approach and assumptions

Table 1. Dissolution Rate Constants, Arrhenius Activation Energies, and Reaction Orders with Respect to H⁺ Activity for Selected Silicate Minerals Reported by Palandri and Kharaka³⁰

mineral	acid mechanism				neutral mechanism ^a		
	pH range ^b	Log rate constant k (mol·m ⁻² ·s ⁻¹)	Arrhenius activation energy, E (kJ·mol ⁻¹)	reaction order n _{H⁺}	pH range ^b	Log rate constant k (mol·m ⁻² ·s ⁻¹)	Arrhenius activation energy, E (kJ·mol ⁻¹)
plagioclase (feldspar/framework silicates)							
albite	1.3–4	−10.2	65.0	0.46	5.6–8.2	−12.6	69.8
anorthite	N/A	−3.50	16.6	1.41	N/A	−9.12	17.8
bytownite	2–5.3	−5.85	29.3	1.02	5.65–7.2	−9.82	31.5
oligoclase	2–4.6	−9.67	65.0	0.46	5.1–7	−11.8	69.8
K feldspar (framework silicates)							
K feldspar	4–5.91	−10.1	51.7	0.50	6–7	−12.4	38.0
orthosilicates							
andradite	N/A	−5.20	94.4	1.00	N/A	−10.7	104
fayalite	N/A	−4.80	94.4	1.00	N/A	−12.8	94.4
forsterite	1.03–8.71	−6.85	67.2	0.47	9.3–12.06	−10.7	79.0
pyroxene and pyroxenoid (chain silicates)							
augite	<~7	−6.82	78.0	0.70	N/A	−12.0	78.0
enstatite	<~7	−9.02	80.0	0.60	N/A	−12.7	80.0
wollastonite	N/A	−5.37	54.7	0.40	N/A	−8.88	54.7
phyllosilicate							
lizardite	N/A	−5.70	75.5	0.80	N/A	−12.4	56.6

^aReaction order n_{H⁺} = 0 for the neutral mechanism because the rate is independent of the pH. ^bThe range corresponds to the data used by Palandri and Kharaka³⁰ to derive each mechanism; in some cases the source did not report the underlying data for some minerals, so the pH range is indicated as N/A.

made) the global capacity until the year 2100 for enhanced rock weathering (ERW) to draw down CO₂ in the form of accumulated pedogenic carbonate ($\omega = 1$) or soluble bicarbonate ($\omega = 2$).

2. MECHANISTIC UNDERPINNINGS OF ERW MODELING IN CROPLANDS

The accumulation of PC and/or enhancement of Alk depends on the speciation of calcium/magnesium ions (M²⁺) with available carbonate and bicarbonate ions (eq 3) and, hence, on the calcium/magnesium release from silicates during silicate dissolution (eq 2). Figure 1 illustrates the fate of silicate weathering in agricultural systems by using wollastonite (CaSiO₃) as an example mineral to illustrate the mechanism. In agricultural soils, silicate dissolution is mainly affected by water conditions (pluvial precipitation and irrigation), soil CO₂ partial pressure (P_{CO₂}), and soil porewater pH. Atmospheric CO₂ enters the soil system via rainwater, thus increasing the concentration of bicarbonate and protons in the system,²³ and the protons govern the silicate dissolution step.⁶ The other sources of soil CO₂ include plant root mass and microbial respiration, as well as organic matter decomposition, thus increasing the near-surface P_{CO₂}.²⁴ Organic acids (tartaric, oxalic, maleic, and citric acids) released as root exudates, microbial decay of plant litter, and secretions from mycorrhizal symbionts (lichen acid, uronic acid, peptides, and amino acids) also lead to soil acidification.^{25,26} Hence, an increase in soil P_{CO₂} as a result of atmospheric CO₂ and plant root exudates results in an increase in silicate dissolution.

P_{CO₂} in soils also depends on the temperature, as seen in Figure 1; soil P_{CO₂} is highest for warm and wet regions experiencing higher rainfall and lowest for cold regions.^{23,24}

Plant growth is higher in warm and wet climates, thus, the soil acidification is higher. Hence, silicate weathering reactions are potentially most rapid in regions with high temperatures and high rainfall. Whereas temperature controls the kinetics of chemical reactions, water is critical to enable the silicate weathering reaction; therefore, warmer and wetter conditions should lead to a higher weathering rate in soils. There exists a strong relation between mineral weathering and wetness according to a complex study investigated recently by Calabrese and Porporato²⁷ to illustrate the role of wetness on the global weathering rate. Rainfall also decides the fate of the formed PC (calcite in the case of wollastonite weathering) and transport of Alk, which will eventually migrate to the ocean (eq 4).

As a result of the increased carbonic acid in the soil, because of heavy rainfall and/or high temperature, the bicarbonates and protons can lead to weathering of the innate SIC already present in the soil naturally, which releases bicarbonates and calcium ions.⁶ Hence, both local climate (rainfall and temperature) and natural carbonate weathering influence the soil acidity; thus, soil pH is the most important controlling factor in silicate weathering and subsequent SIC accumulation. Soils with lower pH are strongly associated with croplands having less innate SIC (thus, more capacity to accumulate PC), having higher rainfall (thus, greater likelihood of SIC migration to the subsoil and aquifers), and having a greater microbial activity (which can aid in leaching silicate minerals²⁸). The ideal soil pH for most plant growth is in the range of 5.0–7.0;²⁹ thus, the basicity of silicate minerals can also help correct the pH of overly acidic soils while undergoing weathering. Hence, the silicate type and application rate chosen for soil amendment applications should be such that contributes to maintaining the favorable pH requirement for these steps: silicate dissolution, calcite precipitation, and plant growth. To

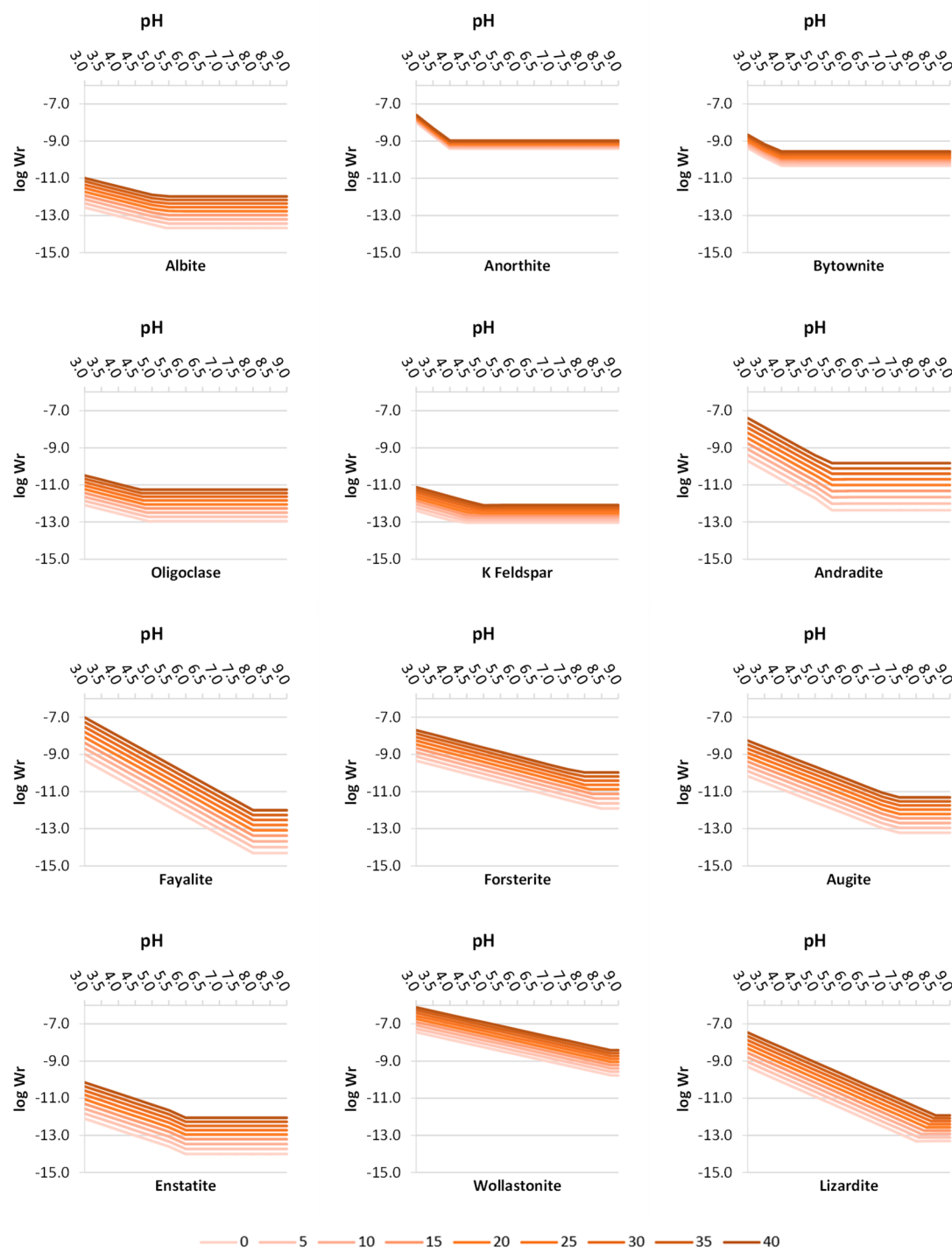


Figure 2. Variation in calculated weathering rate [W_r , $\log(\text{mol} \cdot \text{m}^{-2} \cdot \text{s}^{-1})$] as a function of pH (3.0 to 9.0) and temperature (0 to 40 °C, in order of lighter to darker line shade in 5 °C increments) for 12 silicate minerals (ordered from top left to bottom right according to the classification in Table 1). The W_r acidic (inclined portion) and neutral (horizontal portion) mechanisms were joined as a single line by intersecting them at the pH value where the two calculated W_r values are equal.

emphasize the importance of soil pH on silicate weathering on a global scale and, thus, understand the capacity of global cropland soils and subsoils to accumulate PC/Alk, in this study, we focused on estimating the amount of CO₂ sequestration possible via terrestrial enhanced weathering as a function of soil pH and soil temperature.

3. MODELING OF ERW ON GLOBAL CROPLANDS

3.1. Adopting a Weathering Rate Model. We utilized the widely cited weathering rates of different alkaline minerals from the data made available by Palandri and Kharaka.³⁰ First, Log A [Arrhenius pre-exponential factor at $T = 25$ °C (298.15 K), $\text{mol} \cdot \text{m}^{-2} \cdot \text{s}^{-1}$] is calculated using eq 5, and then the weathering rate is calculated using eq 6 as a function of pH and

temperature. The equation coefficients k , E , and n for both acid mechanism (pH range \sim 3–6) and neutral mechanism (pH range \sim 6–9) are given in Table 1, where k is a calculated rate constant at $T = 25\text{ }^{\circ}\text{C}$ and $\text{pH} = 0\text{ (mol}\cdot\text{m}^{-2}\cdot\text{s}^{-1})$, E is the Arrhenius activation energy ($\text{kJ}\cdot\text{mol}^{-1}$), and n_{H^+} is the reaction order with respect to H^+ . Unlike reported in recent literature by Swoboda et al.,⁹ k or $\log(k)$ should not be used as a comparative proxy for weathering rates of minerals since it is an equation fitting parameter (a rate equation constant) that Palandri and Kharaka³⁰ determined on the basis of regression analysis of large data sets. It does not have sufficient physical significance other than to represent what the weathering rate of a mineral might be at $\text{pH} = 0$, but that is an extrapolation of the pH range used to generate these fitted equation parameters. It is, therefore, critical to compare W_r values of different minerals at the pH and temperature of interest, as next reported.

$$\log A = \log k + \frac{E \times 1000}{2.3025 \times 8.314 \times 298.15} \quad (5)$$

$$\log W_r = \log A - \frac{E \times 1000}{2.3025 \times 8.314 \times T} - n_{\text{H}^+} \times \text{pH} \quad (6)$$

The data reported by Palandri and Kharaka³⁰ is the most widely information used by researchers to understand mineral dissolution, and a common misconception regarding this data, as in Swoboda et al.,⁹ is misinterpreting the rate constant (k) as being or being proportional to a mineral's weathering rate (W_r). For this reason, we hereafter provide the weathering rate values of the minerals listed in Table 1 in a way that can be directly used by the scientific community for comparative analysis and CO_2 sequestration estimation. The variation of the weathering rates, as a function of pH (3.0 to 9.0) and temperature (0 to $40\text{ }^{\circ}\text{C}$) of 12 silicate minerals that are often considered as being potentially suitable for ERW are graphically represented in Figure 2.

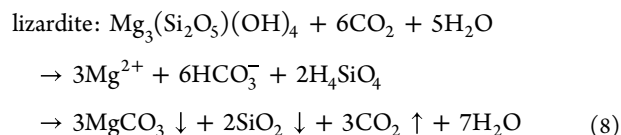
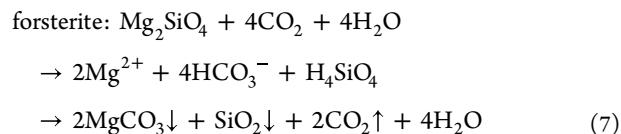
The alkaline minerals with greater (i.e., less negative) logarithmic weathering rate values, e.g., wollastonite (inosilicate), have higher dissolution rates than, e.g., forsterite (orthosilicate belonging to olivine group). It is also evident that acidic soil pH and higher temperature favor the weathering rate for these minerals. It should be noted that the acidic and neutral mechanisms were plotted as a continuous function, but this was only possible by intersecting the two mechanisms at a pH value (for each temperature) where the rates calculated from both mechanisms are equal. Without this data treatment, a step change between the two mechanisms would occur.³¹ It is noted from Figure 2 that, with the intersection approach, the change from one mechanism to the other (sloped to horizontal) occurs at more acidic pH for 7 of the 12 minerals [including anorthite ($\text{CaAl}_2\text{Si}_2\text{O}_8$) and enstatite]. Conversely, for the other five minerals (most notably for forsterite, wollastonite, and lizardite), the slope change happens above a pH of 7. Because of this, the pH-independent neutral mechanism is dominant for the former minerals in the typical pH ranges of global soils, and hence, the weathering rates of the latter minerals are more reliable for the analysis of the present study.

It is possible that some of the underlying data of Palandri and Kharaka³⁰ are less reliable or generated differently than other studies used to build their data sets, so this could explain why some minerals have such a large disconnect (step)

between the two mechanisms.³¹ Some limitations of those data could include various factors of experimental design, such as an inconsistent grinding of rocks that can produce different particle sizes for different minerals, and while weathering rates are normalized per unit surface area, powder samples can have the same surface area even if they have different particle size distributions.³² Additionally, Palandri and Kharaka³⁰ state that the rate equation does not account for the temperature dependence of the pre-exponential factor (A) resulting from variation in the velocity of dissolved species in solution nor does it account for the apparent pH dependence of the activation energy (E). Such discrepancies and limitations call for further experimental investigation of the weathering rates of most of the 12 minerals herein examined to generate more reliable models in the typical pH range of soils (moderately acidic to neutral). Still, the rate values obtained from the model of Palandri and Kharaka³⁰ provide a basis for the investigation of the remainder of this perspective on how ERW interacts with global cropland soil pH.

3.2. CDR Model for ERW on Global Croplands. The CDR for a specific land area, equivalent to the amount of CO_2 removed from the atmosphere by terrestrial enhanced weathering, is determined by taking into consideration the expected soil pH and soil temperature of the cropland, along with the weathering rate of the silicate mineral planned to be used.

The mineral should preferably be available locally, as life cycle analysis by Lefebvre et al.³³ has shown that transportation over more than several hundred kilometers (could be thousands, depending on the mode of transport) significantly reduces the net CO_2 sequestration of ERW. The study of Moosdorf et al.⁷ considered the global availability of suitable rocks for ERW, with a focus on ultramafic rocks (rich in forsterite). Beerling et al.⁸ selected basalt (rich in anorthite) as the global mineral of choice in their study of the potential of ERW because of the wide occurrence of basalt over the Earth's upper crust. In this perspective, we have assumed global availability of each of the minerals exemplified because we aimed to highlight the effects of cropland soil pH and temperature rather than mineral availability, but this is certainly an assumption that should be reviewed on a case-by-case (i.e., region-by-region) basis. We selected wollastonite (CaSiO_3), forsterite (Mg_2SiO_4), and lizardite [$\text{Mg}_3(\text{Si}_2\text{O}_5)_4(\text{OH})_4$] for our analysis as these represent minerals with both demonstrated suitability for ERW in crop soils^{16,34–37} and mine tailings^{2,38,39} scenarios and a diverse set of comparatively fast, moderate, and slow weathering rates (Figure 2), respectively. Anorthite, a common constituent of basalt, was not selected because it was aforementioned that its data in Figure 2 is less reliable. Below is the reaction stoichiometry assumed in calculating the resulting CO_2 sequestration as soluble bicarbonate or as precipitated carbonate:



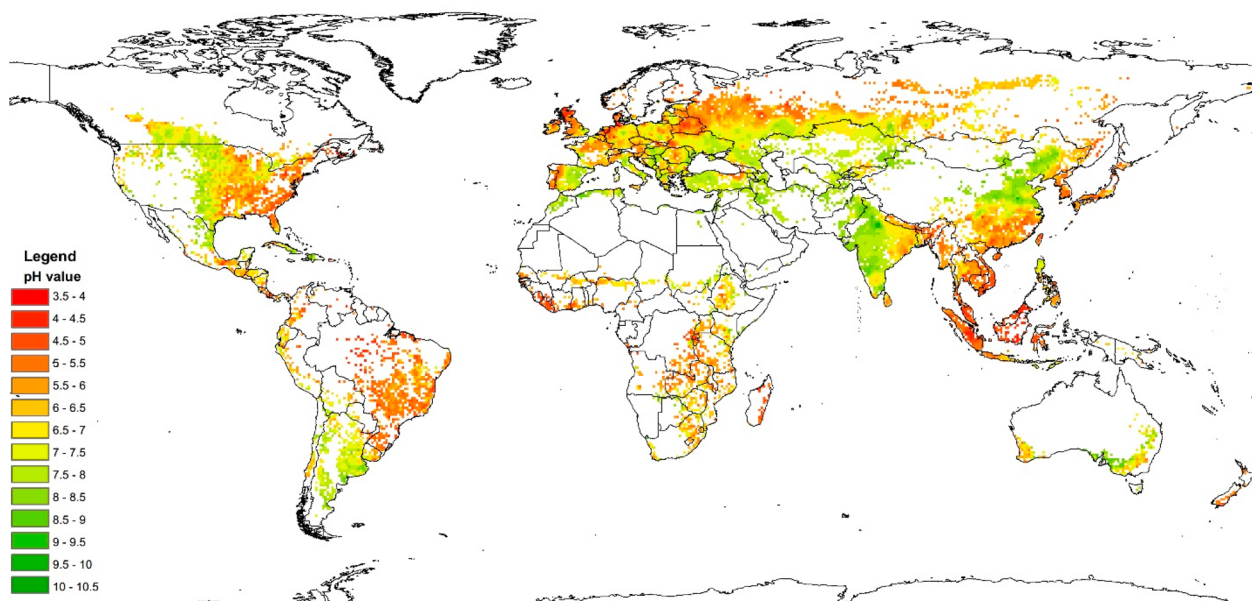


Figure 3. World map of soil pH of cropland areas generated on the basis of pH and location data obtained from the World Soil Information Service⁴⁰ and the United States Geological Survey.⁴¹

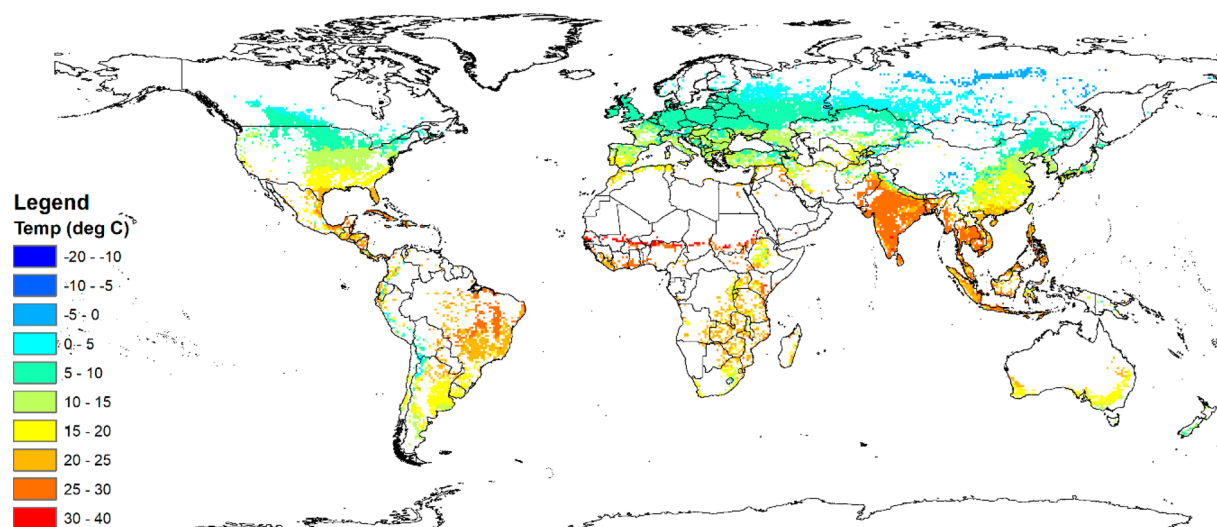
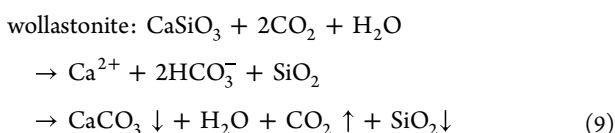


Figure 4. World map of soil temperature (0–50 cm) of cropland areas generated on the basis of temperature and location data obtained from Lembrechts et al.⁴⁴



In our model, it was necessary to know the time taken (t) to reach 100% silicate dissolution/weathering for any given mass of silicate mineral applied to soil in a given year. This was determined using the shrinking core model (eq 10), where initial particle diameter (D_0) was assumed to be 100 μm (or 0.0001 m), and V_m is the molar volume of the mineral (3.983×10^{-5} , 4.408×10^{-5} , and 1.0736×10^{-4} $\text{m}^3 \cdot \text{mol}^{-1}$ for wollastonite, forsterite, and lizardite, respectively). Then, the value of t (in years) for which the conversion $X(t)$ reaches 1 was determined using eq 11. It was further considered that 1 tonne per hectare per year would be the baseline rate of silicate application (as such, the results presented are scalable to the

application tonnage that may be most appropriate for a given mineral, e.g., 5 $\text{tonne} \cdot \text{ha}^{-1} \cdot \text{y}^{-1}$ for wollastonite, 10 $\text{tonne} \cdot \text{ha}^{-1} \cdot \text{y}^{-1}$ for olivine, etc.) and that applications would be done yearly from 2023 to 2100, thereby covering a period of 78 years.

$$X(t) = \frac{D_0^3 - (D_0 - 2W_rV_m t)^3}{D_0^3} \quad (10)$$

$$t = \frac{D_0}{2W_rV_m} \quad \text{at 100\% dissolution} \quad (11)$$

The next step in our CDR model was to generate a world map for cropland soil pH (Figure 3) and the corresponding cropland areas for each pH increment (0.5), and this was accomplished using data from the World Soil Information Service⁴⁰ and the United States Geological Survey.⁴¹ The weathering rates (W_r) and times to dissolution (t) for the three selected minerals were determined using eq 6 over the soil pH

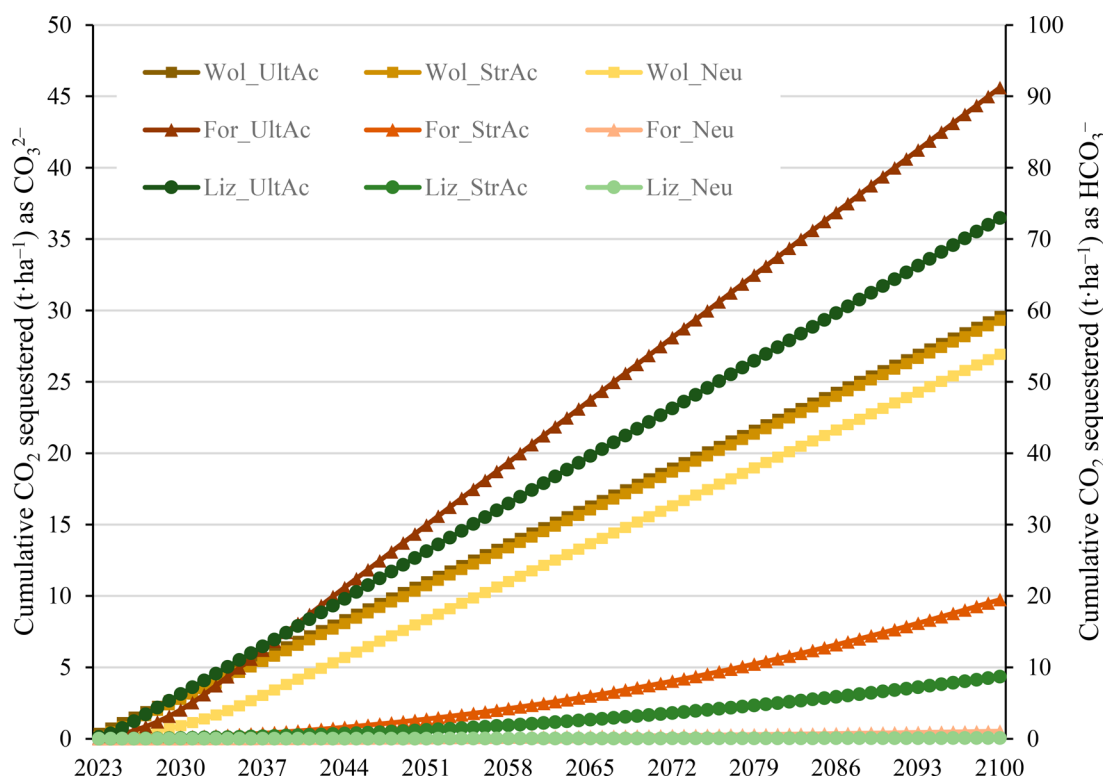


Figure 5. Trend in the cumulative CO_2 sequestered [as pedogenic carbonates (left axis) or as soluble bicarbonate/alkalinity (right axis)] over a period of 78 years, from 2023 to 2100, at ultra-acidic (3.25), strongly acidic (5.25), and neutral (7.25) soil pH for three silicate minerals [wollastonite (Wol), forsterite (For), and lizardite (Liz)] applied at a rate of 1 $\text{tonne} \cdot \text{ha}^{-1} \cdot \text{y}^{-1}$ with an assumed uniform particle size of 100 μm and corresponding soil temperature (22.5, 15, and 7.5 $^\circ\text{C}$) for each pH value. A version of this graph with log-scale, for better visualization of slow weathering scenarios, is given in Figure S2 in the Supporting Information.

range of 3.5 to 8.0 (taking the median pH of each 0.5 increment, i.e., 3.75, 4.25, 4.75, ..., 7.75). Given that crops do not respond well to overly alkaline soils and given that alkaline silicates increase the pH of soils,^{28,34} global cropland regions with a soil pH higher than 8.0 (Figure 3) were excluded from our CDR calculations because they may not be considered for ERW deployment.

One more consideration in our CDR model was the selection of suitable temperature values for use in eq 6. Evidently, surface temperatures vary considerably around the world, even on an annual mean basis. Furthermore, temperatures most relevant for ERW are soil temperatures within the first ~ 0.5 m of depth, and even these temperatures experience diurnal variation (i.e., day/night)⁴² that is predicted to be exacerbated by 2100 because of the ongoing trend of global warming and climate change.⁴³ The annual average soil temperature data was retrieved from Lembrechts et al.,⁴⁴ and the corresponding soil temperature data of global croplands areas were extracted using GIS ArcMap software (Figure 4 and Figure S1 in the Supporting Information). Weathering rates (W_r) and times to dissolution (t) were determined for small temperature intervals (considering the midpoint of 5 $^\circ\text{C}$ intervals, e.g., 2.5 $^\circ\text{C}$ for the 0–5 $^\circ\text{C}$ interval, 27.5 $^\circ\text{C}$ for the 25–30 $^\circ\text{C}$ interval, and 33.5 $^\circ\text{C}$ for the highest interval), and soils with a mean temperature below -5 $^\circ\text{C}$ were disregarded. The total amount of dissolved mineral for each continent was calculated as the sum of mineral dissolved according to our CDR model for each combination of soil pH and soil temperature interval and the percent land area that each such interval represented in the continent.

CDR modeling at the global scale has been previously reported in the literature. For example, Strelfer et al.²⁰ estimated the CDR rates of forsterite and basalt rocks on the basis of a single-dose amendment amount of 150 $\text{tonne} \cdot \text{ha}^{-1}$ and divided global cropland area into warm and temperature regions, where the temperature effect was accounted for as a fixed scaling factor of a standard weathering rate value (i.e., the weathering rate was not determined precisely for the specific soil pH and soil temperature at each global microregion). Beerling et al.⁸ presented a CDR model on the basis of basalt using an amendment rate of 40 $\text{tonne} \cdot \text{ha}^{-1} \cdot \text{y}^{-1}$ and a one-dimensional vertical reactive transport model for rock weathering with steady-state flow that considered soil pH and soil temperature values. However, the article does not clearly present the input data used (e.g., the areal resolution as visualized in our Figures 3 and 4) nor the calculation approach contained in its unpublished Matlab code, and the CO_2 drawdown data is provided for a selection of 12 countries. Our CDR model and perspective looked to expand CO_2 drawdown for all continents on the basis of clearly presented input data (Figures 2–5 and Figure S1). In addition, our CDR model normalizes the amendment rate to 1 tonne per hectare per year over the next 78 years (until 2100), thereby allowing for scaling on the basis of intended liming practices on an agronomic need basis. Finally, the availability of silicate minerals varies worldwide; therefore, it is advantageous to investigate the potential of other candidates of ERW (e.g., lizardite and forsterite) for drawing down CO_2 . The value is modelling the ERW of various silicates while taking into account soil and climate conditions so that it is also then

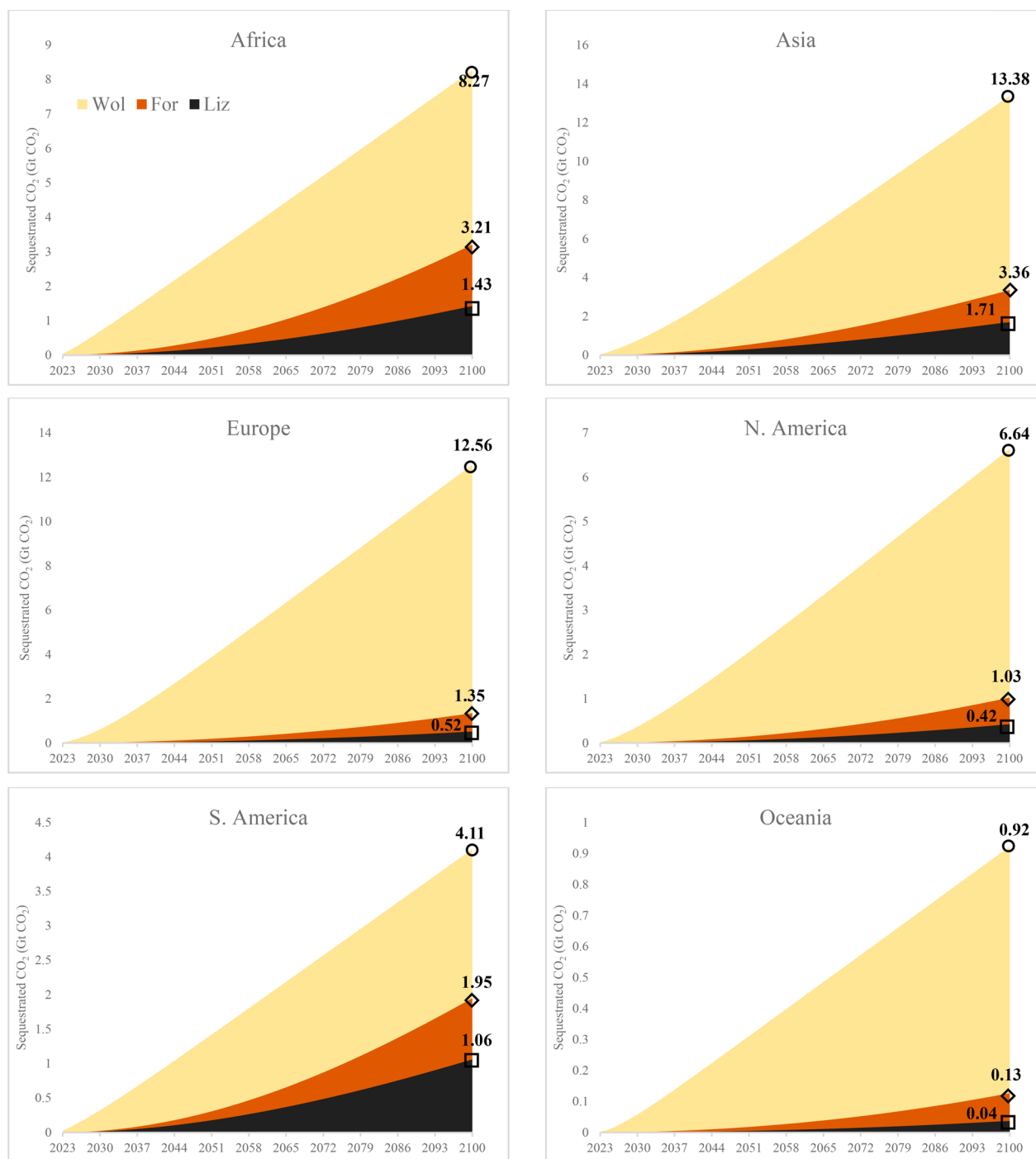


Figure 6. Calculated amount of CO₂ sequestered cumulatively between 2023 and 2100 (Gt of CO₂) according to our CDR model with the application rate of 1 tonne·ha⁻¹·y⁻¹ [as pedogenic carbonates ($\omega = 1$); amounts can increase by as much as double if bicarbonate formation is assumed and no degassing is considered ($\omega = 2$)]. The circle, diamond, and square symbols are indicative of the cumulative amount of sequestered CO₂ at 2100 for wollastonite, forsterite, and lizardite, respectively.

possible to determine what global regions are more suitable for more abundant but slower weathering silicates and what regions would benefit most from the use of less abundant but faster weathering minerals.

3.3. CDR Modeling of ERW on Global Croplands.

3.3.1. Comparison of CO₂ Drawdown Rates Per Hectare as f(pH, T_{soil}). Before we discuss the global cropland model results, we present the weathering dynamics predicted by the model at three different soil pH values: 3.25 (ultra-acidic), 5.25 (strongly acidic), and 7.25 (neutral). The temperatures of 22.5,

15, and 7.5 °C were considered for ultra-acidic, strongly acidic, and neutral classifications, respectively. The selected temperatures are associated with the highest portions of global cropland areas at the given pH ranges on the basis of our calculations (Figure S1). By tracking the age of each applied tonne over the study period and, thus, its dissolution/weathering extent (X) and by considering the CO₂ drawdown capacity of each mineral (0.3793, 0.6255, and 0.1599 tonnes of CO₂ per tonne of mineral for wollastonite, forsterite, and lizardite, respectively, as solid carbonate; double these values as

soluble bicarbonate), the cumulative CO₂ sequestered over time was determined for two scenarios of forming carbonate and bicarbonate (according to eqs 3 and 4). These modeling results are presented in Figure 5.

For ultra-acidic soil pH (3.25), forsterite is shown to capture more CO₂ compared with wollastonite and lizardite, primarily since one mole of forsterite can sequester two moles of CO₂ (as carbonate, eq 7) because of the two magnesium ions present in the chemical formula of forsterite. However, one mole of lizardite can potentially sequester three moles of CO₂ (as carbonate, eq 8) but overall capture less CO₂ compared with forsterite primarily because of its lower weathering rate at the given pH and secondarily because of its lower CO₂ uptake potential (since it possesses more mineral components that do not participate in carbonation reaction). However, at strongly acidic soil pH (5.25) and neutral pH (~7), wollastonite is shown to capture a higher amount of CO₂ compared with both forsterite and lizardite, and this is mainly because of its higher weathering rate at the given soil pH. Accordingly, the weathering rate is recognized as the key parameter that governs the potential of ERW in combating climate change when a deadline is set (i.e., 2100 in this study).

It should be noted that to meet climate mitigation targets in the 100s of megatonnes to gigatonnes per year, amendment rates of multiples of 1 tonne·ha⁻¹·y⁻¹ may be used, but as Figure 5 suggests, slow weathering minerals would accumulate unreacted on croplands, and this could have detrimental effects that are yet to be studied. For example, at high dosages, Haque et al.³⁴ found detrimental effects on plants with wollastonite-amended soils, which can be partly attributed to an excessive increase in soil pH but also to effects that amended minerals can have on soil porosity and sorption of plant nutrients (especially P), among other concerns. Another consideration with regard to amendment rate is that in the calculations used in this study, the silicate application rate pertains to tonnes of the desired mineral; however, in the natural rocks, these minerals are not present in pure form and occur as a mixed composition. For example, forsterite and fayalite are two mineral components of olivine solid solution, and their relative abundance depends on the source of the rock,⁴⁵ while wollastonite mineral is commonly associated with diopside (CaMgSi₂O₆) mineral [which can be associated with hedenbergite (CaFe₂Si₂O₆) in solid solution] as individual phases in natural skarns.⁴⁶ As such, to reach CO₂ drawdowns calculated in this study, the annual amount of rock spreading may need to be twice or thrice the assumed values. This can negatively affect net CO₂ drawdown when emissions from processing and transportation are accounted for,⁸ and excessive traffic of heavy vehicles on farm soils is known to contribute to soil compaction, which affects infiltration,⁴⁷ and consequently can have weathering effects in addition to agronomic impacts.

Figure 5 also demonstrates the rate of CO₂ sequestration in the form of bicarbonate in the soil–water system (which is stoichiometrically two times higher compared with carbonate formation). This suggests that as long as silicate minerals weather in soils, the mobile product (bicarbonate) can find its way through rivers and groundwater to the oceans whereby carbonate and bicarbonate sinks can coexist, and studies have shown that soils and groundwater systems possess sufficient capacity to carry the excess SIC from ERW.^{48,49} A key parameter requiring scientific clarity is on the assumed HCO₃⁻ versus CO₃²⁻ drawdown efficiency factor (here termed ω) in the final (or long-term) sinks of ERW. In our calculations, we

have used both the conservative $\omega = 1$ (for the pedogenic carbonate-only assumption, where each mol of alkaline earth metal uptakes one mol of CO₂) and the maximal $\omega = 2$ (for the soluble bicarbonate-only assumption, where each mol of alkaline earth metal uptakes two mols of CO₂), but there are suggestions that for MRV (monitoring, verification and reporting) purposes, values such as 1.4–1.7 may be appropriate.⁵⁰ For such purposes, should the value of ω be determined locally, regionally, or globally?

3.3.2. Continental CO₂ Drawdown Rates. Finally, the CDR potential of terrestrial silicate weathering for the six continents (North and South America, Europe, Asia, Africa, and Oceania) were estimated, as depicted in Figure 6. As expected, but now quantified, all continents denote the same trend for the potentiality of minerals to sequester carbon with the following order: wollastonite, forsterite, and lizardite. Asia and Europe (noting that all of Russia is considered in Europe for this analysis) exhibit the highest potential to sequester CO₂ when looking at the values for wollastonite because the vast croplands in these continents with suitable conditions for ERW explain the higher potentiality of storing CO₂. However, Asia's drawdown potential for the two more abundant minerals is higher because of greater areas of croplands with soils that are more acidic and warmer. Subtropical and temperate regions experience high levels of dryness, including large parts of North and South America, Africa, and Oceania (which includes Australia), thus explaining the lower CO₂ potential for these continents (compared with Asia and Europe) for wollastonite. Among these regions, however, Africa is a standout for its potential to weather forsterite and lizardite relatively quickly, which contributes to the second highest drawdown potentials of these two minerals (behind Asia). In humid regions, there is more pluvial precipitation, thus leading to soil acidity that is favorable for the weathering rates, while in dry regions, such as desert and semidesert regions, low water availability along with a poor presence of vegetation and low soil organic matter is less favorable for silicate weathering,⁵¹ and Africa and Asia possess vast regions of both climatic conditions.

A possible surprise among these results are the moderate drawdown potentials for South America compared with Africa, but this is explained by the larger cropland of the latter (288 Mha for Africa vs 145 Mha for South America), and the somewhat larger fraction of croplands in Africa having more acidic and warmer soils, while South America has a larger proportion of croplands with alkaline and colder soils (Figure S1). Both continents account for the largest share of cropland expansion in the last two decades (2003–2019), with Africa's growth (+34%) coming primarily from the conversion of natural vegetation and tree plantations, while South America's growth (+49%) is primarily tied to the replacement of pastures and the recultivation of abandoned agricultural lands.⁵²

It is important to also note that our CDR model does not account for other pertinent soil properties that may affect the weathering rate of silicate minerals, such as soil type, vegetation type, management practices, soil fertilization, hydrological conditions, and soil microbial activities.⁸ The CO₂ sequestration amounts presented in Figure 6 could be further constrained on the basis of these factors, including more certainty on the regional or global ω values to be assumed in such models, and this should be the focus of future studies. For instance, Dietzen and Rosing⁵² have recently proposed using a correction factor for accounting the effect of noncarbonic acid on ERW CO₂ uptake (i.e., the ω value).

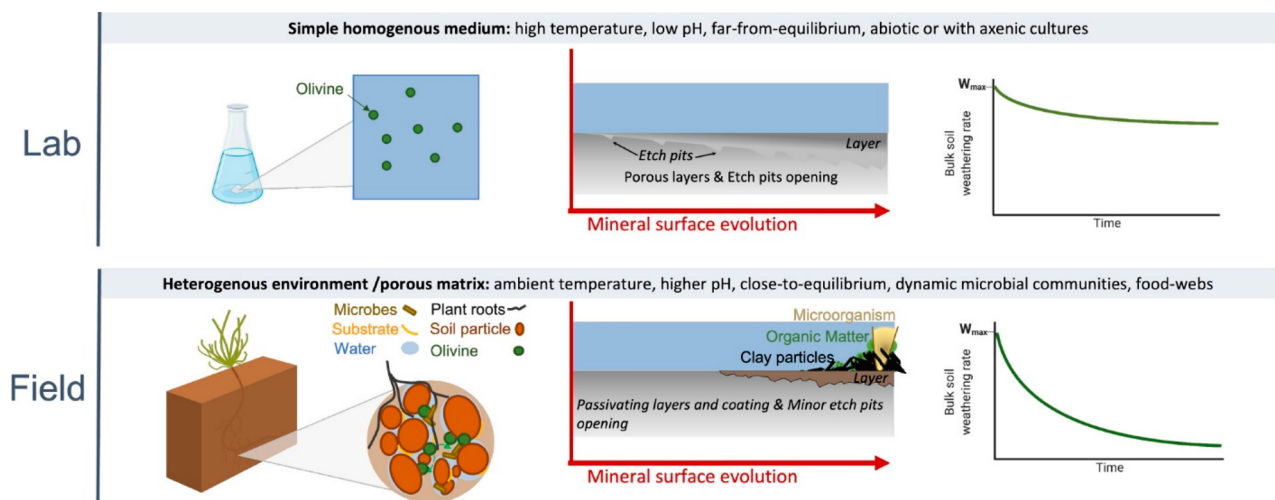


Figure 7. Comparison between laboratory and field weathering environments, the corresponding evolution of the mineral surface area, and the resulting evolution of weathering rates (shown conceptually). Reprinted with permission from Calabrese et al.⁵³ Copyright 2022 American Chemical Society.

Another important factor in our analysis is the source of the weathering rates. Calabrese et al.⁵³ and earlier authors have discussed that laboratory-based weathering rates can substantially differ from those in the field. However, not enough studies are available in the context of ERW versus in the context of natural weathering. In a recent study of olivine weathering over two years in microplots of soil with pH = 6.0, a W_r value of $7.43 \times 10^{-11} \text{ mol} \cdot \text{m}^{-2} \cdot \text{s}^{-1}$ was reported,⁵⁴ which is within the range of T -dependent values presented in Figure 2 for pH 6.0. While it is possible that the illustration from Calabrese et al.⁴⁹ in Figure 7 is qualitatively a reasonable representation of the lab versus field comparison, not enough is known to make quantitative assessments of how different these rates are over time and how the passivation mechanism can also limit full conversion [$X(t) \rightarrow 1$] of the minerals (as assumed in our model). Such understanding will only be possible once multiyear field trials yield reliable data that tracks all forms of sequestered CO₂ (i.e., pedogenic carbonates, alkalinity, organo–mineral complexes, and total soil organic carbon). As such, the CO₂ sequestration values found in our study represent an upper limit of (i.e., constrain) the possible contribution of ERW as a negative emissions technology.

4. CONCLUDING REMARKS AND OUTLOOK

The relation between cropland soil pH and soil temperature (and other factors) and ERW CO₂ sequestration potential investigated in this study sheds light on the mechanism through which these parameters affect the silicate weathering rate at a global scale. The spatial distribution of the world's croplands over diverse climatic and geologic zones, which impacts their potential to form and accumulate SIC to aid in CO₂ sequestration, highlights the importance of accounting for regional soil pH and soil temperature in modeling studies that aim to estimate carbon dioxide sequestration potential via mineral weathering. The spatial representation of weathering rates and cumulative CO₂ drawdown helps us to identify the regions that are more suitable for slower and faster weathering silicate soil amendments, and this should be balanced with the availability of suitable minerals (natural or waste-derived) within reasonable transport distances, the types of crops grown in those regions and their soil health and nutrient require-

ments, and the selection of mineral amendment rates that correspond to agronomic benefits in addition to climate change mitigation targets.

■ ASSOCIATED CONTENT

SI Supporting Information

The Supporting Information is available free of charge at <https://pubs.acs.org/doi/10.1021/acsearthspacechem.2c00374>.

Figure S1, the percentage of cropland area within each temperature interval on the basis of pH values for each continent, and Figure S2, the logarithmic trend in the cumulative CO₂ sequestered (PDF)

■ AUTHOR INFORMATION

Corresponding Author

Rafael M. Santos — School of Engineering, University of Guelph, Guelph, Ontario N1G 2W1, Canada; orcid.org/0000-0002-8368-8618; Email: santosr@uoguelph.ca

Authors

Fatima Haque — School of Engineering, University of Guelph, Guelph, Ontario N1G 2W1, Canada; Department of Bioenvironmental Systems Engineering, National Taiwan University, Taipei 10617, Taiwan
 Reza Khalid — School of Engineering, University of Guelph, Guelph, Ontario N1G 2W1, Canada
 Yi Wai Chiang — School of Engineering, University of Guelph, Guelph, Ontario N1G 2W1, Canada

Complete contact information is available at:
<https://pubs.acs.org/10.1021/acsearthspacechem.2c00374>

Author Contributions

[§]F.H. and R.K. contributed equally. The manuscript was written through the contributions of all authors. All authors have approved the final version of the manuscript. F.H.: Methodology, Formal analysis, Investigation, Writing—Original Draft. R.K.: Methodology, Formal analysis, and Investigation. Y.C.: Conceptualization, Methodology, Writing—Review and Editing, Supervision, and Funding acquisition.

R.S.: Conceptualization, Methodology, Resources, Supervision, Project administration, and Funding acquisition.

Funding

This work was funded by the Ontario Agri-Food Innovation Alliance (Gryphon's LAAIR Product Development grant UG-GLPD-2021-101200), Natural Sciences and Engineering Research Council of Canada (Discovery Grant 401497), and Canada First Research Excellence Fund (Food from Thought Product Development grant 499149).

Notes

The authors declare no competing financial interest.

ACKNOWLEDGMENTS

The authors would like to thank Hesam Salmabadi at the Université du Québec à Trois-Rivières for helping with the geospatial data analysis of this study. The authors acknowledge the financial support provided by the Ontario Agri-Food Innovation Alliance, the Natural Sciences and Engineering Research Council of Canada, and the Canada First Research Excellence Fund.

ABBREVIATIONS

Alk, alkalinity; CDR, carbon dioxide removal; ERW, enhanced rock weathering; PC, pedogenic carbonate; P_{CO_2} , soil CO_2 partial pressure; SIC, soil inorganic carbon

REFERENCES

- (1) Canadell, J. G.; Le Quéré, C.; Raupach, M. R.; Field, C. B.; Buitenhuis, E. T.; Ciais, P.; Conway, T. J.; Gillett, N. P.; Houghton, R. A.; Marland, G. Contributions to Accelerating Atmospheric CO_2 Growth from Economic Activity, Carbon Intensity, and Efficiency of Natural Sinks. *Proc. Natl. Acad. Sci. U. S. A.* **2007**, *104* (47), 18866–18870.
- (2) Khalidy, R.; Santos, R. M. The Fate of Atmospheric Carbon Sequestered through Weathering in Mine Tailings. *Miner. Eng.* **2021**, *163*, 106767.
- (3) IPCC. *Climate Change 2021: The Physical Science Basis. Contribution of Working Group I to the Sixth Assessment Report of the Intergovernmental Panel on Climate Change*; Cambridge University Press: Cambridge, United Kingdom and New York, NY, 2021; pp 159–254.
- (4) Fuss, S.; Lamb, W. F.; Callaghan, M. W.; Hilaire, J.; Creutzig, F.; Amann, T.; Beringer, T.; de Oliveira Garcia, W.; Hartmann, J.; Khanna, T.; et al. Negative Emissions—Part 2: Costs, Potentials and Side Effects. *Environ. Res. Lett.* **2018**, *13* (6), 63002.
- (5) Lackner, K. S. A Guide to CO_2 Sequestration. *Science* **2003**, *300* (5626), 1677–1678.
- (6) Hartmann, J.; West, A. J.; Renforth, P.; Köhler, P.; De La Rocha, C. L.; Wolf-Gladrow, D. A.; Dürr, H. H.; Scheffran, J. Enhanced Chemical Weathering as a Geoengineering Strategy to Reduce Atmospheric Carbon Dioxide, Supply Nutrients, and Mitigate Ocean Acidification. *Rev. Geophys.* **2013**, *51* (2), 113–149.
- (7) Moosdorf, N.; Renforth, P.; Hartmann, J. Carbon Dioxide Efficiency of Terrestrial Enhanced Weathering. *Environ. Sci. Technol.* **2014**, *48* (9), 4809–4816.
- (8) Beerling, D. J.; Kantzas, E. P.; Lomas, M. R.; Wade, P.; Eufrasio, R. M.; Renforth, P.; Sarkar, B.; Andrews, M. G.; James, R. H.; Pearce, C. R.; et al. Potential for Large-Scale CO_2 Removal via Enhanced Rock Weathering with Croplands. *Nature* **2020**, *583* (7815), 242–248.
- (9) Swoboda, P.; Döring, T. F.; Hamer, M. Remineralizing Soils? The Agricultural Usage of Silicate Rock Powders: A Review. *Sci. Total Environ.* **2022**, *807*, 150976.
- (10) Hangx, S. J. T.; Spiers, C. J. Coastal Spreading of Olivine to Control Atmospheric CO_2 Concentrations: A Critical Analysis of Viability. *Int. J. Greenh. Gas Control* **2009**, *3* (6), 757–767.
- (11) Monger, H. C.; Kraimer, R. A.; Khresat, S.; Cole, D. R.; Wang, X.; Wang, J. Sequestration of inorganic carbon in soil and groundwater. *Geology* **2015**, *43* (5), 375–378.
- (12) Köhler, P.; Hartmann, J.; Wolf-Gladrow, D. A. Geoengineering Potential of Artificially Enhanced Silicate Weathering of Olivine. *Proc. Natl. Acad. Sci. U. S. A.* **2010**, *107* (47), 20228–20233.
- (13) Dietrich, F.; Diaz, N.; Deschamps, P.; Sebag, D.; Verrecchia, E. P. Calcium transfer and mass balance associated with soil carbonate in a semi-arid silicate watershed (North Cameroon): An overlooked geochemical cascade? *Depositional Rec.* **2021**, *7*, 93–110.
- (14) Kwon, S.; Fan, M.; DaCosta, H. F. M.; Russell, A. G. Factors Affecting the Direct Mineralization of CO_2 with Olivine. *J. Environ. Sci.* **2011**, *23* (8), 1233–1239.
- (15) Lackner, K. S.; Wendt, C. H.; Butt, D. P.; Joyce Jr, E. L.; Sharp, D. H. Carbon Dioxide Disposal in Carbonate Minerals. *Energy* **1995**, *20* (11), 1153–1170.
- (16) Haque, F.; Santos, R. M.; Chiang, Y. W. CO_2 Sequestration by Wollastonite-Amended Agricultural Soils-An Ontario Field Study. *Int. J. Greenhouse Gas Control* **2020**, *97*, 103017.
- (17) Georgakopoulos, E.; Santos, R. M.; Chiang, Y. W.; Manovic, V. Influence of Process Parameters on Carbonation Rate and Conversion of Steelmaking Slags-Introduction of the ‘Carbonation Weathering Rate. *Greenh. Gases Sci. Technol.* **2016**, *6* (4), 470–491.
- (18) Zhang, N.; Santos, R. M.; Siller, L. Rapid CO_2 capture-to-mineralisation in scalable reactor. *Reaction Chemistry & Engineering* **2020**, *5* (3), 473–484.
- (19) Cipolla, G.; Calabrese, S.; Porporato, A.; Noto, L. V. Effects of precipitation seasonality, irrigation, vegetation cycle and soil type on enhanced weathering - modeling of cropland case studies across four sites. *Biogeosciences* **2022**, *19*, 3877–3896.
- (20) Strelfer, J.; Amann, T.; Bauer, N.; Kriegler, E.; Hartmann, J. Potential and Costs of Carbon Dioxide Removal by Enhanced Weathering of Rocks. *Environ. Res. Lett.* **2018**, *13* (3), 034010.
- (21) Rinder, T.; von Hagke, C. The influence of particle size on the potential of enhanced basalt weathering for carbon dioxide removal - Insights from a regional assessment. *Journal of Cleaner Production* **2021**, *315*, 128178.
- (22) Haque, F.; Chiang, Y. W.; Santos, R. M. Alkaline Mineral Soil Amendment: A Climate Change ‘Stabilization Wedge’? *Energies* **2019**, *12* (12), 2299.
- (23) Marotta, H.; Duarte, C. M.; Pinho, L.; Enrich-Prast, A. Rainfall leads to increased pCO_2 in Brazilian coastal lakes. *Biogeosciences* **2010**, *7* (5), 1607–1614.
- (24) Hashimoto, S.; Komatsu, H. Relationships between Soil CO_2 Concentration and CO_2 Production, Temperature, Water Content, and Gas Diffusivity: Implications for Field Studies through Sensitivity Analyses. *J. For. Res.* **2006**, *11* (1), 41–50.
- (25) Epiphov, D. Z.; Batterman, S. A.; Hedin, L. O.; Leake, J. R.; Smith, L. M.; Beerling, D. J. N₂-Fixing Tropical Legume Evolution: A Contributor to Enhanced Weathering through the Cenozoic? *Proc. R. Soc. B Biol. Sci.* **2017**, *284* (1860), 20170370.
- (26) Pokrovsky, O. S.; Shirokova, L. S.; Bénédith, P.; Schott, J.; Golubev, S. V. Effect of Organic Ligands and Heterotrophic Bacteria on Wollastonite Dissolution Kinetics. *Am. J. Sci.* **2009**, *309* (8), 731–772.
- (27) Calabrese, S.; Porporato, A. Wetness Controls on Global Chemical Weathering. *Environ. Res. Commun.* **2020**, *2* (8), 85005.
- (28) Haque, F.; Santos, R. M.; Chiang, Y. W. Optimizing Inorganic Carbon Sequestration and Crop Yield With Wollastonite Soil Amendment in a Microplot Study. *Front. Plant Sci.* **2020**, *11*, 1012.
- (29) Atiyeh, R. M.; Subler, S.; Edwards, C. A.; Bachman, G.; Metzger, J. D.; Shuster, W. Effects of Vermicomposts and Composts on Plant Growth in Horticultural Container Media and Soil. *Pedobiologia (Jena)* **2000**, *44* (5), 579–590.
- (30) Palandri, J. L.; Kharaka, Y. K. *A Compilation of Rate Parameters of Water-Mineral Interaction Kinetics for Application to Geochemical Modeling, USGS Open File Report 2004–1068*; U.S. Geological Survey: Menlo Park, CA, 2004.

- (31) Haque, F.; Khalidy, R.; Chiang, Y. W.; Santos, R. Role of Local Climate, Innate SIC Content, and Soil pH on Amended Mineral Weathering Rates and Capacity to Accumulate Pedogenic Carbonates in Croplands. *16th Greenhouse Gas Control Technologies Conference 2022 (GHGT-16)*, October 23–25, 2022. DOI: [10.2139/ssrn.4277725](https://doi.org/10.2139/ssrn.4277725).
- (32) Dudhaiya, A.; Santos, R. M. How characterization of particle size distribution pre- and post-reaction provides mechanistic insights into mineral carbonation. *Geosciences* **2018**, *8* (7), 260.
- (33) Lefebvre, D.; Goglio, P.; Williams, A.; Manning, D. A. C.; de Azevedo, A. C.; Bergmann, M.; Meersmans, J.; Smith, P. Assessing the potential of soil carbonation and enhanced weathering through Life Cycle Assessment: A case study for Sao Paulo State, Brazil. *J. Cleaner Prod.* **2019**, *233*, 468–481.
- (34) Haque, F.; Santos, R. M.; Dutta, A.; Thimmanagari, M.; Chiang, Y. W. Co-Benefits of Wollastonite Weathering in Agriculture: CO₂ Sequestration and Promoted Plant Growth. *ACS Omega* **2019**, *4* (1), 1425–1433.
- (35) Khalidy, R.; Haque, F.; Chiang, Y. W.; Santos, R. M. Monitoring Pedogenic Inorganic Carbon Accumulation Due to Weathering of Amended Silicate Minerals in Agricultural Soils. *J. Visualized Exp.* **2021**, *172*, No. e61996.
- (36) ten Berge, H. F. M.; van der Meer, H. G.; Steenhuizen, J. W.; Goedhart, P. W.; Knops, P.; Verhagen, J. Olivine Weathering in Soil, and Its Effects on Growth and Nutrient Uptake in Ryegrass (*Lolium perenne* L.): A Pot Experiment. *PLoS One* **2012**, *7* (8), No. e42098.
- (37) Renforth, P.; Pogge von Strandmann, P. A. E.; Henderson, G. M. The dissolution of olivine added to soil: Implications for enhanced weathering. *Appl. Geochem.* **2015**, *61*, 109–118.
- (38) Embile Jr, R. F.; Walder, I. F.; Mahoney, J. J. Forsterite and pyrrhotite dissolution rates in a tailings deposit obtained from column leaching experiments and inverse modeling: A novel method for a mine tailings sample. *Appl. Geochem.* **2018**, *98*, 65–74.
- (39) Power, I. M.; Paulo, C.; Long, H.; Lockhart, J. A.; Stubbs, A. R.; French, D.; Caldwell, R. Carbonation, Cementation, and Stabilization of Ultramafic Mine Tailings. *Environ. Sci. Technol.* **2021**, *55* (14), 10056–10066.
- (40) International Soil Reference and Information Centre (ISRIC). *WoSIS latest - pH H₂O data*. 2020. <https://data.isric.org/geonetwork/srv/eng/catalog.search#/metadata/44e9cac5-2cb7-41c3-9fb0-0bc8b716e993> (accessed 2021-10-28).
- (41) United States Geological Survey (USGS). *Cropland by Continent*. <https://www.usgs.gov/media/images/cropland-continent> (accessed 2021-12-28).
- (42) Zhang, H.; Liu, B.; Zhou, D.; Wu, Z.; Wang, T. Asymmetric Soil Warming under Global Climate Change. *Int. J. Environ. Res. Public Health* **2019**, *16* (9), 1504.
- (43) Bradford, J. B.; Schlaepfer, D. R.; Lauenroth, W. K.; Palmquist, K. A.; Chambers, J. C.; Maestas, J. D.; Campbell, S. B. Climate-Driven Shifts in Soil Temperature and Moisture Regimes Suggest Opportunities to Enhance Assessments of Dryland Resilience and Resistance. *Front. Ecol. Evol.* **2019**, *7*, 358.
- (44) Lembrechts, J. J.; van den Hoogen, J.; Aalto, J.; Ashcroft, M. B.; De Frenne, P.; Kemppinen, J.; Kopecký, M.; Luoto, M.; Maclean, I. M. D.; Crowther, T. W.; et al. Global Maps of Soil Temperature. *Glob. Chang. Biol.* **2022**, *28* (9), 3110–3144.
- (45) Buseck, P. R.; Goldstein, J. I. Olivine Compositions and Cooling Rates of Pallasic Meteorites. *Geol. Soc. Am. Bull.* **1969**, *80* (11), 2141–2158.
- (46) Grammatikopoulos, T. A.; Clark, A. H. A comparative study of wollastonite skarn genesis in the Central Metasedimentary Belt, southeastern Ontario, Canada. *Ore Geology Reviews* **2006**, *29* (2), 146–161.
- (47) Nawaz, M. F.; Bourrié, G.; Trolard, F. Soil compaction impact and modelling. A review. *Agron. Sustain. Dev.* **2013**, *33*, 291–309.
- (48) Zhang, S.; Planavsky, N. J.; Katchinoff, J.; Raymond, P. A.; Kanzaki, Y.; Reershemius, T.; Reinhard, C. T. River Chemistry Constraints on the Carbon Capture Potential of Surficial Enhanced Rock Weathering. *Limnol. Oceanogr.* **2022**, *67*, S148–S157, DOI: [10.1002/limo.12244](https://doi.org/10.1002/limo.12244).
- (49) Khalidy, R.; Arnaud, E.; Santos, R. M. Natural and Human-Induced Factors on the Accumulation and Migration of Pedogenic Carbonate in Soil: A Review. *Land* **2022**, *11* (9), 1448.
- (50) Renforth, P.; Henderson, G. Assessing ocean alkalinity for carbon sequestration. *Rev. Geophys.* **2017**, *55*, 636–674.
- (51) Potapov, P.; Turubanova, S.; Hansen, M. C.; Tyukavina, A.; Zalas, V.; Khan, A.; Song, X.-P.; Pickens, A.; Shen, Q.; Cortez, J. Global maps of cropland extent and change show accelerated cropland expansion in the twenty-first century. *Nat. Food* **2022**, *3*, 19–28.
- (52) Dietzen, C.; Rosing, M. T. Quantification of CO₂ uptake by enhanced weathering of silicate minerals applied to acidic soils. *Int. J. Greenhouse Gas Control* **2023**, *125*, 103872.
- (53) Calabrese, S.; Wild, B.; Bertagni, M. B.; Bourg, I. C.; White, C.; Aburto, F.; Cipolla, G.; Noto, L. V.; Porporato, A. Nano- to Global-Scale Uncertainties in Terrestrial Enhanced Weathering. *Environ. Sci. Technol.* **2022**, *56* (22), 15261–15272.
- (54) Vink, J. P. M.; Giesen, D.; Ahlrichs, E. Olivine weathering in field trials - Effect of natural environmental conditions on mineral dissolution and the potential toxicity of nickel; Deltares: Utrecht, The Netherlands, 2022. https://publications.deltares.nl/11204378_000_0002.pdf (accessed 2023-05-18).